Microchannel fabrication on cyclic olefin polymer substrates via 1064 nm Nd:YAG laser ablation

Ronán McCann[a, b, c, d], Komal Bagga[a, b, c], Robert Groarke[a, b, c], Apryll Stalcup[c, e], Mercedes Vázquez[a, c, e, *], Dermot Brabazon[a, b, c, d]

[a]Advanced Processing Technology Research Centre, Dublin City University, Glasnevin, Dublin 9, Ireland

[b]School of Mechanical and Manufacturing Engineering, Dublin City University, Dublin 9, Ireland

[c]Irish Separation Science Cluster, National Centre for Sensor Research, Dublin City University, Dublin 9, Ireland

[d]National Centre for Plasma Science and Technology, Dublin City University, Dublin 9, Ireland

[e]School of Chemical Sciences, Dublin City University, Dublin 9, Ireland

---

***Corresponding Author:**

Dr. Mercedes Vázquez

School of Chemical Sciences,

Dublin City University, Dublin 9, Ireland

Tel: + 353 1 700 7602

Fax: + 353 1 700 5503

E-mail: mercedes.vazquez@dcu.ie

Abstract

This paper presents a method for fabrication of microchannels on cyclic olefin polymer films that have application in the field of microfluidics and chemical sensing. Continuous microchannels were fabricated on 188-µm-thick cyclic olefin polymer substrates using a picosecond pulsed 1064 nm Nd:YAG laser. The effect of laser fluence on the microchannel morphology and dimensions was analysed via scanning electron microscopy and optical profilometry. Single laser passes were found to produce v-shaped microchannels with depths ranging from 12 to 48 µm and widths from 44 to 154

µm. The ablation rate during processing was lower than predicted theoretically. Multiple laser passes were applied to examine the ability for finer control over microchannel morphology with channel depths ranging from 22 µm to 77 µm and channel widths from 59 µm to 155 µm. For up to five repeat passes, acceptable reproducibility was found in the produced microchannel morphology. Infrared spectroscopy revealed that the polymer surface chemistry was not significantly altered via the laser ablation process. These results were compared to other work conducted on cyclic olefin polymers.

Keywords: Laser ablation; cyclic olefin polymer; microchannel fabrication; Nd:YAG; picosecond; microfluidics

1. Introduction

Until recently, the typical materials of choice for microfluidic devices and micro-total analysis systems have been glass or polymers such as polymethyl methacrylate (PMMA), polycarbonate (PC), and polydimethylsiloxane (PDMS). These materials have good mechanical properties, allowing for easy processing but often lack good optical transparency in the mid-ultraviolet spectrum (200 – 300 nm). Optical transparency in this range is crucial for the optical analysis of many organic compounds such as aromatics, proteins and nucleic acids. Cyclic-olefin polymer (COP) and co-polymer (COC) are an emerging new classes of polymers which have been noted for their low cost, high chemical resistance, biocompatibility and high optical transparency from NIR to mid-UV wavelengths [1]. COPs are also recognized for their low water absorption and high mechanical and dimensional stability when in contact with liquids, and as such make extremely suitable platforms for microfluidic devices when compared with previously used alternatives. Owing to these exceptional properties, COP-based devices have been utilised for various applications such as substrates for chromatographic stationary phases [2] and microfluidic devices for the analysis of drugs [3], IR waveguide coatings [4] and as substrates for laser deposited nanomaterials [5].

For microfluidic device fabrication, techniques such as xurography [6], micromilling [7], UV-polymerisation [8] and, more recently, 3D printing [9,10] allow for fast and flexible prototyping of

devices leading to shorter periods to device optimisation. For large-scale fabrication of devices, techniques such as hot embossing [11] or injection moulding [12] tend to be used due to their cost-effectiveness. However, these lack the ability for rapid prototyping due to the requirement of moulds or negatives to be fabricated. Contrastingly, laser processing provides a fast, repeatable, clean and cost efficient method of microfluidic device manufacturing. The use of laser processing [13,14] and pulsed laser ablation [15] has been demonstrated to be capable of both surface modification and creation of micro- and nanoscale structures on polymer surfaces, along with the incorporation of nanoparticles onto the substrate surface for functionalisation and nanotexturing [16].

Neodymium-doped yttrium aluminium garnet (Nd:YAG) lasers are widely used in industry for materials processing [17], however, very few studies have examined the feasibility of using Nd:YAG lasers for the processing of cyclic olefin polymers [6]. Various alternative laser systems, such as ultra-violet and extreme ultra violet laser systems and femtosecond lasers, have been utilized for polymer processing in the past. UV excimer lasers have been used for the processing of optically transparent polymers [18], and specifically COC [19]. The low ablation depth per pulse for COC, which was found to be smaller when compared to PMMA, would allow for the creation of small features although the extent of ablation was seen to be dependent on the norbornene content of the copolymer [20]. However, UV excimer lasers tend to have higher operating cost and lower beam quality when compared to solid-state laser systems. Extreme ultraviolet (EUV) lasers, typically used in microelectronics manufacturing, have also been shown to be capable of nanoscale changes in depth and surface roughness of polymer surfaces due to low penetration depth of EUV radiation [21,22]. Despite these advantages, EUV lasers require a vacuum and highly specialised optics for operation and therefore are not well suited for the fabrication of low-cost microfluidic systems.

Femtosecond lasers, which interact with materials through non-linear photon absorption, have been demonstrated for the efficient processing of materials transparent to the wavelength of the laser used [15]. For COP processed using a femtosecond titanium sapphire (800 nm) laser, low surface roughness of the processed area was reported [23]. However, some degradation in optical transmission was seen due to a combination of oxidation and dehydrogenation when compared with

PMMA or polystyrene (PS) processed under the same conditions. While fast delivery of power by femtosecond lasers allows for efficient processing of materials transparent to the wavelength of the laser, these systems tend to be both more expensive and complicated to maintain than laser processing systems typically used in industry.

In this work, we examine the use of an infrared picosecond pulsed Nd:YAG laser for direct-write fabrication of continuous microchannels on the surface of thin COP substrates. The use of multiple laser passes for fine control of dimensions and dimensional uniformity was also examined. Optical profilometry was used for dimensional analysis of the microchannels and scanning electron microscopy was performed to analyse changes in surface morphology. Raman and infrared spectroscopy were performed to examine the effect of laser processing on the surface chemistry.

2. Material and Methods

2.1 Materials

The substrate material used was ZeonorFilm ZF14-188 (Zeon) cyclic olefin polymer purchased from Ibidi, Germany, with a thickness of 188 µm. The polymer sheet was cut, cleaned with isopropanol, rinsed with deionised water and dried using compressed clean dry air to ensure the substrate was pristine prior to laser processing.

2.2 Laser processing and substrate fabrication

The direct-write laser system used consisted of a 1064 nm Q-switched, diode-pumped solid-state neodymium-yttrium aluminium garnet laser (BrightSolutions 1064 WEDGE HF), specifications of which are listed in Table 1. A 2D scanning galvanometer (Raylase SS-12) was used to raster the beam in the xy-plane, and a movable z-stage (PI M-404 4PD) was used to control the position of the sample. The laser beam was focussed to a spot size of 140 µm and scanned unidirectionally across the sample at a speed of 1.2 mm/s to form parallel channels separated by 200 µm. The COP films were mechanically fastened to the sample stage for the duration of processing. Further details of the processing parameters are listed in Table 2.

107 **Table 1.** Specifications of the 1064 nm laser processing system.

Wavelength	1064 nm
Maximum Average Output Power	4.5 W
Maximum Pulse Energy	45 mJ
Repetition Rate	7.5 – 100 kHz
Pulse width	0.7 – 5.2 ns
Beam diameter	140 µm

108

109

110 **Table 2:** Process parameters used during laser processing of COP substrates.

Process Parameter	Single Pass	Multiple Passes
Fluence	0.15 – 0.78 J/cm^2	0.51 J/cm^2
Scan Rate (mm/s)	1.2	1.2
Beam diameter (µm)	140	140
Pulse Width (ps)	750	750
Pulse Repetition Frequency (kHz)	7.5	7.5
No. of passes	1	2 to 10

111

112 *2.3 Characterisation*

113 Scanning electron microscopy was conducted using an EVO LS15 (Zeiss) with LaB_6 filament,
114 accelerating voltage of 10 kV, and a beam current intensity of 25 pA. Samples were gold coated using
115 a ScanCoat Six (Edwards) sputter coater set at a deposition current of 25mA for 80 s, resulting in a
116 coating thickness of 34 nm.

117 The profile of the microchannels was examined using a VHX-2000 (Keyence) 3D Optical
118 Microscope. Samples were previously coated with a 68-nm-thick film of gold using the ScanCoat Six

sputter coater, which was sufficient to reduce the transmission in the visible range by approximately 90% [24] and allow the sample surface to be imaged optically. Images were taken at 0.43 µm increments upwards from the base of the channel at 1000x magnification. For the figures presented hereafter, the error bars relate to a 90% confidence interval of the measured microchannels width and depth.

The optical absorbance of the polymer film at the laser wavelength was examined using a Cary 50 (Varian) UV-Vis spectrometer. Infrared spectroscopy was performed to examine changes to the substrate surface chemistry as a result of laser processing. Micro-Raman spectroscopy was conducted using a LabRam HR800 (Jobin-Yvon Horiba) system with an Ar^+ 488 nm air-cooled laser and an accumulation time of 20 s. The HR800 was operated in a backscattering configuration with a resolution of 1.1 cm^{-1}. FTIR spectroscopy was performed using a Perkin 100 spectrometer (PerkinElmer) in attenuated total reflectance (ATR) mode. A baseline correction was applied to the FTIR spectra using Origin Pro 9, to allow accurate comparison of relative peak intensities.

2.4 Calculation of ablation rate

The number of laser pulses, *N,* incident per unit area in a scanning beam can be estimated from the laser pulse repetition frequency, *f*, the beam waist, w_0, and scan rate, *v*, as follows [25]:

$$N = w_0 f / v \tag{1}$$

This will then allow determination of the experimental ablation rate, R_m, i.e. the amount of material removed per pulse, which can be estimated as the measured channel depth, *d*, divided by *N*:

$$R_m = d/N \tag{2}$$

For the parameters used in this work, a value of 875 pulses per unit area of a laser pass was calculated from Equation 1. Theoretical ablation rates, R_t, i.e. the expected amount of material removed per pulse, can be calculated using

$$R_t = \alpha^{-1} \cdot \ln(F/F_{th}) \tag{3}$$

where F and F_{th} are the input and threshold fluences respectively. The "effective optical penetration depth", α^{-1}, from the *Beer-Lambert law* can be estimated from the slope of the linear fit of a linear-log plot of the ablation depth versus fluence [26]. Predicted microchannel width, W, for an incident fluence of F can be estimated using w_o and F_{th} [26] whereby

$$W^2 = 2w_0^2 \cdot \ln(F/F_{th}) \quad (4)$$

This equation assumes that the microchannel widths are equivalent to a single pulse ablation site rather than a scanning beam of multiple pulses. Some variation from the predicted values is expected as a result of the "incubation effect" [26], whereby defects generated by the interaction of multiple laser shots effectively lower the threshold fluence as the number of laser pulses increases. Despite this, this calculation allows insight into the expected variation between single and multiple scanning passes.

3. Results and Discussion

3.1 Effect of laser fluence

The effect of laser fluence on the formation of microchannels on the substrate surface was investigated from the resultant 3D profiles. Both microchannel widths and depths were seen to increase logarithmically with laser fluence as shown in

Figure 1. At the lowest fluence used (0.23 J/cm^2), microchannels 44 µm wide and 12 µm deep were formed. The highest fluence (0.79 J/cm^2) resulted in microchannels 154 µm in width and 47 µm in depth. The logarithmic increase of channel width with increased fluence reflects the underlying absorption mechanism which itself is logarithmically dependant on the ratio between the incident and transmitted laser intensities. A lower correlation coefficient was obtained when a logarithmic fit was applied to the microchannel depth vs. fluence data, indicating there are other factors affecting microchannel depth at high fluences such as energy adsorption and interruption of the chaotic formation of condensed ablated polymer. At all fluences, microchannels with a V-shaped profile were formed, similar to the findings from other work conducted with COP [23], with re-cast ablation melt

evident at the channel crests which reduced in size at higher fluences. This reduction may be attributed to thermal diffusion from the ablation site causing a localised melting of condensed debris. For the maximum fluence used (0.79 J/cm^2) heat damage was evident through substrate warping and the appearance of large bubble-like formations on the substrate surface. The increased build-up of heat in the processed area at higher fluences would be expected to result in increased levels of damage. The repetitive and localised nature of this damage followed the pattern of the applied laser pulsing.

Figure 2 shows 3D images of the microchannels taken using optical profilometry. For the lower fluence pass (0.34 J/cm^2), a narrow and shallow V-shaped channel with condensed ablated material and melt around the channel edges was observed, see Figure 2a. A wider and deeper microchannel which contained localised deeper ablation sites along the bottom of the channel resulted from the higher fluence pass (0.79 J/cm^2), see Figure 2b.

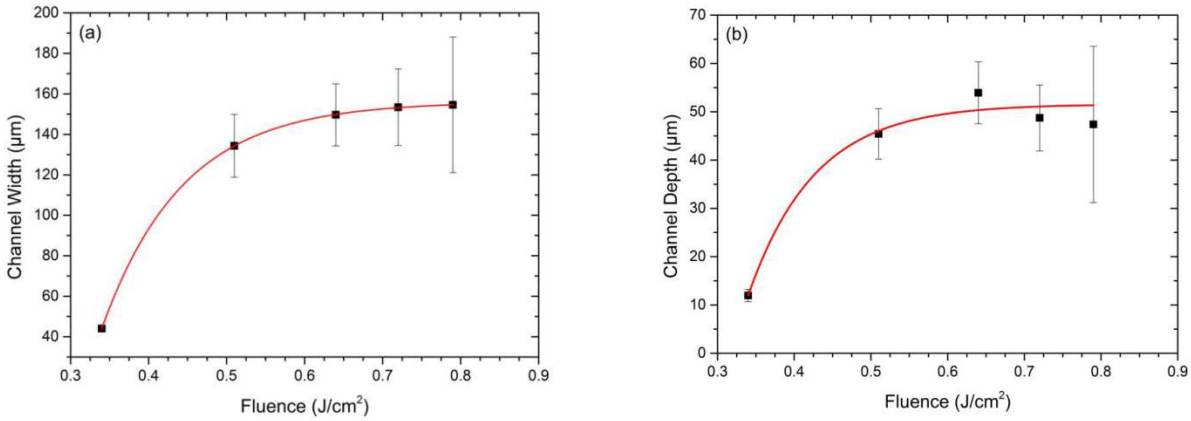

Figure 1. Measured microchannel (a) widths and (b) depths as a function of laser fluence for a single laser pass.

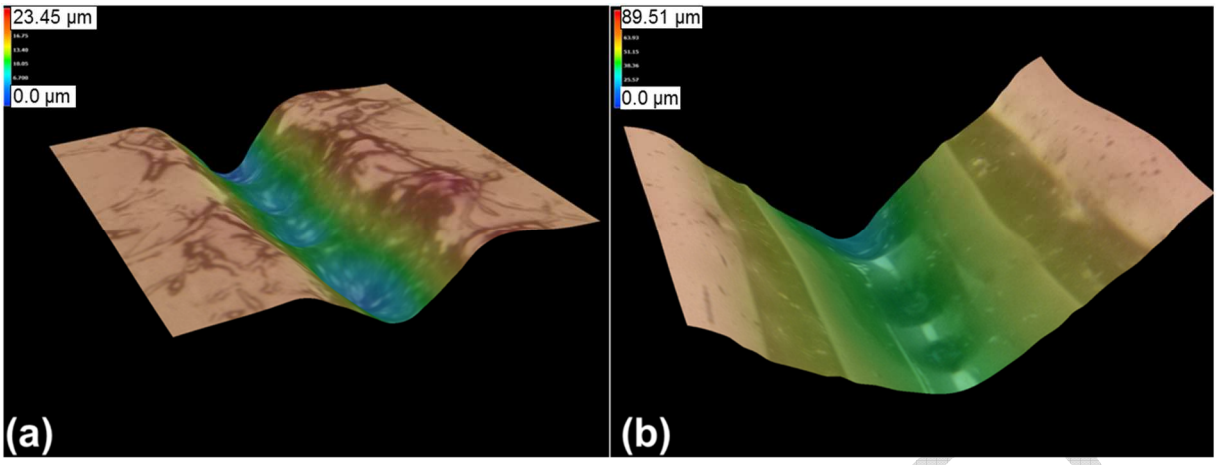

Figure 2. Optical profilometry images of microchannels produced from a single laser pass at a fluence (a) 0.34 J/cm^2 and (b) 0.79 J/ cm^2.

3.2 Ablation Rate

The ablation rate, i.e. the amount of material removed per laser pulse, was calculated to allow for insight into the laser ablation process under experimental conditions. Figure 3 compares the experimental ablation rates (Equation 2) and calculated ablation rates (Equation 3). The threshold fluence (0.32 J/cm^2) used in Equation 3, was estimated from the x-axis intercept in Figure 1b. The effective optical penetration depth, α^{-1}, was determined from the slope of the linear fit applied to data in Figure 1b once plotted on a linear-log scale, and was found to be 140 nm. For low fluences, ablation rates of 17 nm/pulse were recorded, while for higher fluences rates of up to 60 nm/pulse were recorded. These rates were found to be similar to work performed on other grades of cyclic olefin polymers and copolymers. Ablation rates of approximately 60 – 170 nm/pulse using an ArF excimer laser [19] and approximately 20 – 70 nm/pulse using a KrF excimer [20] laser have been observed over a range of laser fluences. The measured ablation rate was seen to plateau after a fluence of 0.64 J/cm^2.

The ablation rate predicted from Equation 1 was higher than that predicted from Equation 3 for fluences greater than 0.72 J/cm^2, while for the highest fluence used (0.79 J/cm^2) the opposite was

found. Equation 1 is based on a theoretical calculation for a single, isolated ablation site. It has been previously discussed that the production of microchannels can result in ablation rates which are higher than expected theoretically due to ablated material being allowed to escape from the previously processed area [25]. Furthermore, as the ablation rate calculation does not incorporate changes in the threshold fluence because of the "incubation effect", some deviation from the theory is expected. These processes would account for the discrepancy seen in Figure 3 for fluences below 0.79 J/cm^2. The lower than predicted ablation rate for a fluence of 0.79 J/cm^2 was attributed to absorption within the laser-generated ablation plume attenuating the laser pulse energy during processing.

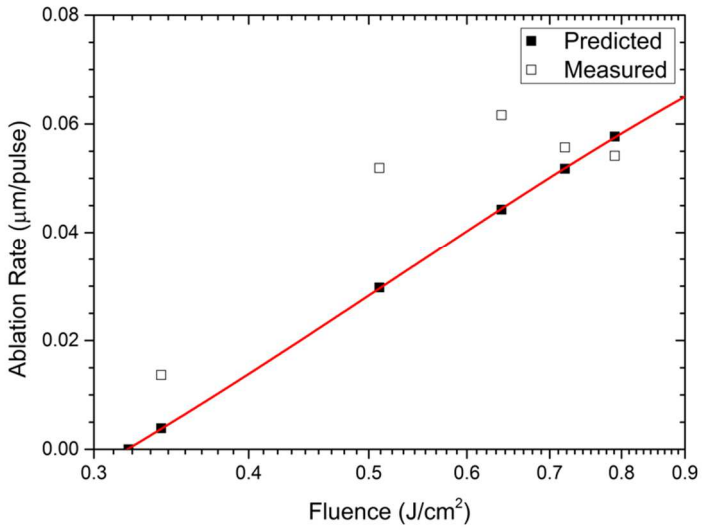

Figure 3. A comparison of the predicted and measured ablation rates for various laser fluences.

3.3 Effect of multiple laser passes

Both microchannel width and depth increased with successive laser passes (Figure 4a and 4b respectively). For microchannel depth, there was a noted decrease in channel reproducibility for seven or more passes along with substrate warping during processing. For seven and eleven passes, debris was evident along the channel walls and crests see Figure 5. This debris became more rounded for higher number of laser passes.

For multiple laser passes, keeping the number of passes at or below five was optimal. This allowed for fine control over the microchannel morphology without a significant decrease in channel reproducibility. This decrease in channel reproducibility above five passes was again attributed to the build-up of heat during processing, as evident by substrate warping, resulting in the substrate surface moving within the laser focal plane. This damage due to build-up of heat at both high fluences and high number of passes highlights the possible need for active cooling of the substrate when high fluence processing is needed. Use of a thicker substrate, which would have a larger thermal mass, could also be a good alternative to minimise this damage.

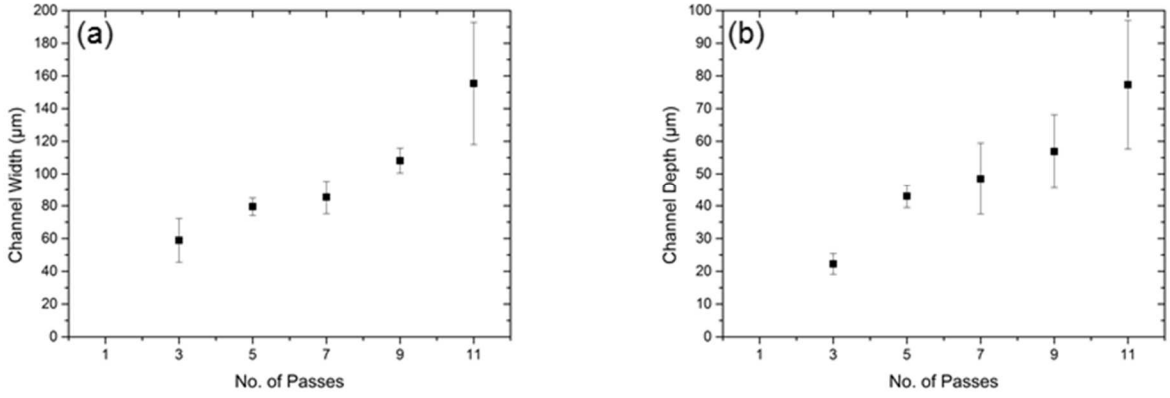

Figure 4. Measured microchannel (a) width and (b) depth as a function of number of laser passes.

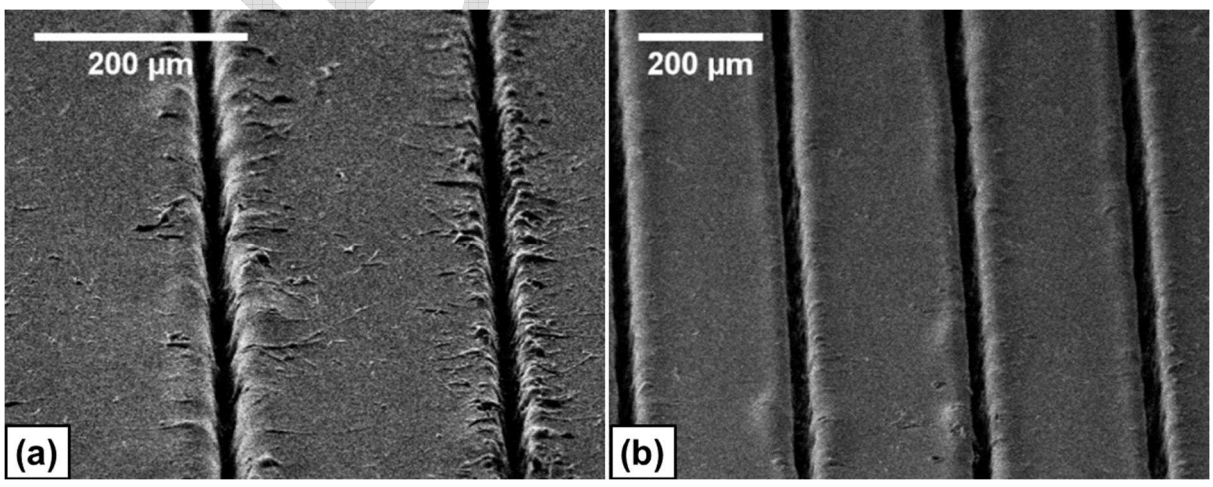

Figure 5. Scanning electron microscopy images of the COP substrate after (a) 7 and (b) 11 laser passes.

3.4 Surface Analysis

Raman and FTIR spectroscopy were performed to study the surface chemical composition after laser processing. The base of the microchannel was examined for changes, while the measurements from the interchannel areas (which were not processed), were used as a reference, as shown in Figure 6a. Both Raman and FTIR (Figure 6b and Figure 7) showed no significant differences in peak position for both the channel and interchannel areas. This indicated that the surface chemistry of the microchannels was not significantly altered by laser processing, thus retaining the chemical resistance and biocompatibility as of the unprocessed COP. Nevertheless, FTIR revealed oxidation after laser processing as evidenced by an increase in IR absorbance at the 1650 – 1750 cm^{-1} range. Dehydrogenation was also evident through a reduction in C-H absorbance at 2800 – 2950 cm^{-1}. The appearance of a broad peak after 3000 cm^{-1} was also observed. These mechanisms of degradation are consistent with that reported for other work on COP [23,27].

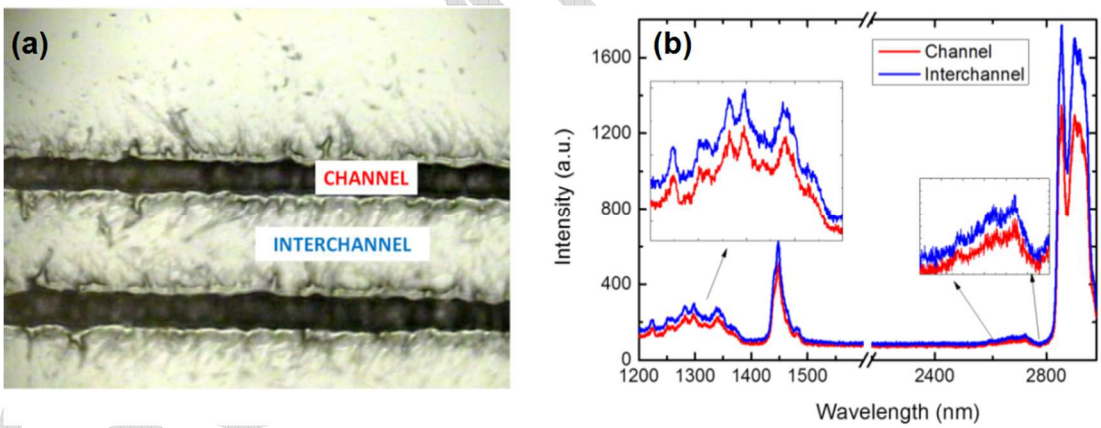

Figure 6: Optical image (a) and micro-Raman spectra (b) of the laser processed COP substrates.

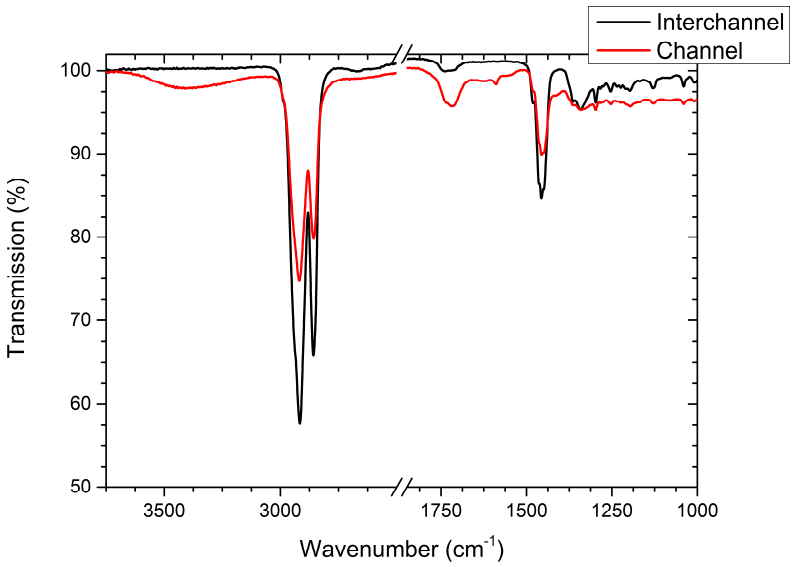

Figure 7: ATR-FTIR spectrum of the COP substrate before and after laser processing.

4. Conclusions

This paper presents the first investigation into laser-texturing of microchannels on cyclic olefin polymer using an industrial 1064 nm Nd:YAG laser. The ability to tailor microchannel depth and width by varying laser fluence was demonstrated. Microchannels between 44 µm and 154 µm width and 12 µm to 47 µm depth were obtained over the fluence range examined. The channels at all fluences presented a V-shape profile. The experimental ablation rate was calculated based on the microchannel depth and the number of incident laser pulses, and was compared to that expected from theory with ablation rates ranging from 13 nm/pulse up to 55 nm/pulse observed.

The use of multiple laser passes for fine-tuning of microchannel morphology was also examined with channel depths ranging from 22 µm to 77 µm and channel widths from 59 µm to 155 µm found. For up to five repeat laser passes, acceptable reproducibility in channel dimensions was observed allowing for finer control over channel depths and widths. However, a large decrease in reproducibility of the microchannel depths occurred for seven passes and above. Both infrared and Raman spectroscopy revealed that the laser processing had not significantly altered the chemical composition of the polymer substrate. However, indications of substrate oxidation and dehydrogenation were seen in the FTIR spectra as expected based on previously reported work on laser processing of cyclic olefin

polymers. Ultimately, this work should allow for quick, single-step fabrication of reproducible microchannels on optically transparent substrates that have applications in lab-on-a-chip and microfluidic devices.

Acknowledgements

This publication has emanated from research conducted with the financial support of Science Foundation Ireland (SFI) under Grant Number 12/IA/1576 and the European Union's Horizon 2020 Research and Innovation Program under the Marie Sklodowska-Curie grant agreement No. 655194. The authors would like to thank Dr. Rajani Vijayaraghavan for assistance with the Raman spectroscopy, and Mr. Vincent Hooper for assistance with the FTIR spectroscopy.

290

291 **References**

292 [1] P.S. Nunes, P.D. Ohlsson, O. Ordeig, J.P. Kutter, Cyclic olefin polymers: Emerging materials
293 for lab-on-a-chip applications, Microfluid. Nanofluidics. 9 (2010) 145–161.

294 [2] K. Faure, M. Albert, V. Dugas, G. Crétier, R. Ferrigno, P. Morin, et al., Development of an
295 acrylate monolith in a cyclo-olefin copolymer microfluidic device for chip
296 electrochromatography separation., Electrophoresis. 29 (2008) 4948–55.

297 [3] Y. Yang, C. Li, J. Kameoka, K.H. Lee, H.G. Craighead, A polymeric microchip with
298 integrated tips and in situ polymerized monolith for electrospray mass spectrometry., Lab
299 Chip. 5 (2005) 869–76.

300 [4] Y.-W. Shi, Y. Wang, Y. Abe, Y. Matsuura, M. Miyagi, H. Uyama, et al., Fabrication of cyclic
301 olefin polymer (COP)-coated silver hollow glass waveguides for the infrared, in: M.S. Bogner,
302 S.T. Charles, W.S. Grundfest, J.A. Harrington, A. Katzir, L.S. Lome, et al. (Eds.), Proc. SPIE,
303 Surgical-Assist Systems, San Jose, CA., USA, 1998: pp. 96–102.

304 [5] S. Inguva, R.K. Vijayaraghavan, E. McGlynn, J.-P. Mosnier, Highly transparent and
305 reproducible nanocrystalline ZnO and AZO thin films grown by room temperature pulsed-
306 laser deposition on flexible Zeonor plastic substrates, Mater. Res. Express. 2 (2015) 096401.

307 [6] A. Ben Azouz, S. Murphy, S. Karazi, M. Vázquez, D. Brabazon, Fast Fabrication Process of
308 Microfluidic Devices Based on Cyclic Olefin Copolymer, Mater. Manuf. Process. 29 (2014)
309 93–99.

310 [7] P.-C. Chen, C.-W. Pan, W.-C. Lee, K.-M. Li, An experimental study of micromilling
311 parameters to manufacture microchannels on a PMMA substrate, Int. J. Adv. Manuf. Technol.
312 71 (2014) 1623–1630.

313 [8] S. Turri, M. Levi, E. Emilitri, R. Suriano, R. Bongiovanni, Direct Photopolymerisation of
314 PEG-Methacrylate Oligomers for an Easy Prototyping of Microfluidic Structures, Macromol.
315 Chem. Phys. 211 (2010) 879–887.

316 [9] X. Zhang, X.. Jiang, C. Sun, Micro-stereolithography of polymeric and ceramic
317 microstructures, Sensors Actuators A Phys. 77 (1999) 149–156.

318 [10] A.I. Shallan, P. Smejkal, M. Corban, R.M. Guijt, M.C. Breadmore, Cost-effective three-
319 dimensional printing of visibly transparent microchips within minutes., Anal. Chem. 86 (2014)
320 3124–30.

321 [11] R.K. Jena, C.Y. Yue, Y.C. Lam, Micro fabrication of cyclic olefin copolymer (COC) based
322 microfluidic devices, Microsyst. Technol. 18 (2011) 159–166.

323 [12] M. Matschuk, H. Bruus, N.B. Larsen, Nanostructures for all-polymer microfluidic systems,
324 Microelectron. Eng. 87 (2010) 1379–1382.

325 [13] J.-Y. Cheng, C.-W. Wei, K.-H. Hsu, T.-H. Young, Direct-write laser micromachining and
326 universal surface modification of PMMA for device development, Sensors Actuators B Chem.
327 99 (2004) 186–196.

328 [14] O. Lyutakov, J. Tůma, I. Huttel, V. Prajzler, J. Siegel, V. Švorčík, Polymer surface patterning
329 by laser scanning, Appl. Phys. B. 110 (2013) 539–549.

330 [15] S. Baudach, J. Bonse, J. Krüger, W. Kautek, J. Kruger, Ultrashort pulse laser ablation of
331 polycarbonate and polymethylmethacrylate, Appl. Surf. Sci. 154-155 (2000) 555–560.

332 [16] V.N. Bagratashvili, N. V. Minaev, A.A. Rybaltovsky, A.O. Rybaltovsky, S.I. Tsypina, V.Y.

333 Panchenko, et al., Laser fabrication of periodic microstructures from silver nanoparticles in
334 polymer films, Laser Phys. 20 (2010) 139–143.

335 [17] S. Prakash, B. Acherjee, A.S. Kuar, S. Mitra, An experimental investigation on Nd:YAG laser
336 microchanneling on polymethyl methacrylate submerged in water, Proc. Inst. Mech. Eng. Part
337 B J. Eng. Manuf. 227 (2013) 508–519.

338 [18] Y.-T. Chen, K. Naessens, R. Baets, Y.-S. Liao, A.A. Tseng, Ablation of Transparent Materials
339 Using Excimer Lasers for Photonic Applications, Opt. Rev. 12 (2005) 427–441.

340 [19] D. Sabbert, J. Landsiedel, H.-D. Bauer, W. Ehrfeld, ArF-excimer laser ablation experiments
341 on Cycloolefin Copolymer (COC), Appl. Surf. Sci. 150 (1999) 185–189.

342 [20] P.W. Leech, Effect of norbornene content on laser ablation of cyclic olefin copolymers,
343 Mater. Des. 31 (2010) 4858–4861.

344 [21] A. Bartnik, H. Fiedorowicz, R. Jarocki, J. Kostecki, M. Szczurek, O. Chernyayeva, et al.,
345 EUV-induced physico-chemical changes in near-surface layers of polymers, J. Electron
346 Spectros. Relat. Phenomena. 184 (2011) 270–275.

347 [22] Inam Ul Ahad, A. Bartnik, H. Fiedorowicz, J. Kostecki, B. Korczyc, T. Ciach, et al., Surface
348 modification of polymers for biocompatibility via exposure to extreme ultraviolet radiation., J.
349 Biomed. Mater. Res. A. 102 (2014) 3298–310.

350 [23] R. Suriano, A. Kuznetsov, S.M. Eaton, R. Kiyan, G. Cerullo, R. Osellame, et al., Femtosecond
351 laser ablation of polymeric substrates for the fabrication of microfluidic channels, Appl. Surf.
352 Sci. 257 (2011) 6243–6250.

353 [24] O. Loebich, The optical properties of gold, Gold Bull. 5 (1972) 2–10.

354 [25] A. Rodríguez, A. Arriola, T. Tavera, N. Pérez, S.M. Olaizola, Enhanced depth control of
355 ultrafast laser micromachining of microchannels in soda-lime glass, Microelectron. Eng. 98
356 (2012) 672–675.

357 [26] A. Ben-Yakar, R.L. Byer, Femtosecond laser ablation properties of borosilicate glass, J. Appl.
358 Phys. 96 (2004) 5316–5323.

359 [27] C. Liu, J. Yu, X. Sun, J. Zhang, J. He, Thermal degradation studies of cyclic olefin
360 copolymers, Polym. Degrad. Stab. 81 (2003) 197–205.

361